THE ARCHIVE OF MECHANICAL ENGINEERING

VOL. LIX 2012 Number 1

10.2478/v10180-012-0004-3

Key words: Multiple Rushton impellers, four blades, six blades, stirred tank, numerical, experimental

ZIED DRISS [*], *SARHAN KARRAY* [*], *WAJDI CHTOUROU* [*], *HEDI KCHAOU* [*], *MOHAMED SALAH ABID* [*]

A STUDY OF MIXING STRUCTURE IN STIRRED TANKS EQUIPPED WITH MULTIPLE FOUR-BLADE RUSHTON IMPELLERS

The effect of multiple Rushton impellers configurations on hydrodynamics and mixing performance in a stirred tank has been investigated. Three configurations defined by one, two and three Rushton impellers are compared. Results issued from our computational fluid dynamics (CFD) code are presented here concerning fields of velocity components and viscous dissipation rate. These results confirm that the multi-impellers systems are necessary to decrease the weaken zones in each stirred tanks. The experimental results developed in this work are compared with our numerical results. The good agreement validates the numerical method.

1. Introduction

Mixing is very important in many industrial applications. For example, in bioreactors motion is responsible for bringing reactants in close contact and in adequate stoichiometry so that biological reactions can occur. These mechanical reactions include biomass production and synthesis of biological products. Also, mixing is responsible for dispersing the synthesised products and these products include the molecule of interest as well as toxic products, inhibitors and secondary products [1]. Depending on the purpose of the operation carried out in the mixer, the best choice for the geometry of the tank and the impeller type can vary widely. Many researches, was focused on the optimisation of the design of the stirred tanks and impellers geometry. For example, Driss et al. [2] developed a computational study of the pitched blade turbines design effect on the stirred tank flow characteristics. Particularly, they studied the effects of different inclined angle, equal to 45°,

[*] *Laboratory of Electro-Mechanic Systems (LASEM), National School of Engineers of Sfax (ENIS), University of Sfax (US), B.P. 1173, Road Soukra, km 3.5, 3038 Sfax, Tunisia; E-mail: Zied.Driss@enis.rnu.tn, Zied_Driss@yahoo.fr*

60° and 75°, on the local and global flow characteristics. Kchaou et al. [3] compared the effect of the flat-blade turbine with 45° and -45°pitched blade turbines on the hydrodynamic structure of the stirred tank. Stitt [4] noted that multiphase reactor designs from larger scale and non-catalytic processes are now being considered. These include trickle beds, bubble columns and jet or loop reactors. Murthy and Joshi [5] tested five impeller designs namely disc turbine, variety of pitched blade down flow turbine impellers varying in blade angle and hydrofoil impeller. Karcz and Major [6] studied the influence of the baffles length in a stirred tank equipped with different types of turbines like the Rushton turbine, the Smith turbine, the pitched blade turbine and the propeller. Placek and Tavlarides [7] presented 2D simulation using the model of discharge flow from a turbine disc. Montante et al. [8] studied the recirculation zone of the flows in the model of transition in a tank agitated by the technique using laser Doppler anemometry (LDA). They studied the influence of the position of the turbine compared to the bottom and the influence of the baffles on the hydrodynamics of the flows in stirred tanks with a Rushton turbine in order to define an optimal position for a maximum axial velocity. Deglon and Meyer [9] investigated the effect of grid resolution and discretization scheme on the CFD simulation of fluid flow in a baffled mixing tank stirred by a Rushton turbine. Pericleous and Patel [10] modelled single and multi stage radial impellers as distributed sources of momentum, on the basis of the blade fluid relative velocity and of drag coefficients taken from the literature. Costes and Couderc [11] studied the fields of the average velocities obtained by the LDV (Laser Doppler Velocimetry) in the plane of the baffles and the median plane of a stirred tank equipped by Rushton turbine. Alcamo et al. [12] computed by large-eddy simulation (LES) the turbulent flow field generated in an unbaffled stirred tank by a Rushton turbine. The Smagorinsky model was used for the unresolved or sub-grid scales. A general purpose CFD code was appropriately modified in order to allow the computation of the sub-grid viscosity and to perform statistics on the computed results. The numerical predictions were compared with the literature results using particle image velocimetry. Zalc et al. [13] explored laminar flow in an impeller stirred tank using CFD tools. They extended the analysis to include short and long time mixing performance as a function of the impeller speed. The simulated flow fields are validated extensively by particle image velocimetry (PIV). Also, they used planar laser induced fluorescence (PLIF) to compare the experimental and computed mixing patterns. Brucato et al. [14] studied the turbulent flow generated by one and two Rushton turbines in different axial positions. They studied the effect of the grid scaling on the assessment of the three velocity components, the turbulent kinetic energy, the dissipation rate and the evolution of power num-

ber. Alvarez et al. [15] studied a stirred tank system with a single Rushton impeller mounted in a central shaft. Using UV visualization techniques, they illustrated the 3D mechanism by which fluorescent dye is dispersed within the chaotic region of the tank. Also, they compared a system of three Rushton impellers with a system having three discs at the same locations. Guillard and Trägardh [16] designed and tested a new model for estimating mixing times in aerated stirred tanks with three reactors which were equipped with two, three and four Rushton impellers. The results showed that the analogy model developed is independent of the scale, the geometry of the tank, the number of impellers used, the distance between impellers and the degree of homogeneity considered. Only the region in which the pulses were added was found to affect the results. Chtourou et al. [17] interested to provide predictions of turbulent flow in a stirred vessel and to assess the ability to predict the dissipation rate of turbulent energy that constitutes a most stringent test of prediction capability due to the small scales at which dissipation takes place. The amplitude of local and overall dissipation rate is shown to be strongly dependent on the choice of turbulence models. Ammar et al. [18] analyzed numerically the effect of the baffles length on the turbulent flows in stirred tanks equipped by a Rushton turbine. The numerical results from the application of the CFD code Fluent with the MRF model are presented in the vertical and horizontal planes in the impeller stream region.

On the basis of the literature review, we can confirm that the literature is very rich by the mechanical stirred tank studies and particularly those equipped by the six-blade Rushton turbine. However, there is lack of some particular system like the multiple four-blade Rushton impellers.

In this paper, CFD modelling has been carried out to compare the fundamental mechanisms of laminar mixing with multiple four-blade Rushton impellers in a vessel tank. We have focused on the low Reynolds number mixing regime because this situation arises in our practical applications. The objective is to understand the fundamental hydrodynamic processes in stirred vessels in order to choose the most effective system.

2. Geometric Arrangement

The geometric arrangement consist of multiple four-blades Rushton impellers in a cylindrical tank with a diameter D equal to height (D=H). The shaft is placed concentrically with a diameter ratio s/D of 0.02. The blade is defined by a height and a width equal to w=0.06 D and l=0.09 D respectively. Agitation was provided with three Rushton turbines of diameter d=D/3 placed at the distance h_1 from the vessel base. Distances between Rushton turbines discs are equal to h_2 and h_3 (Fig. 1). Particularly, we have compared three

different configurations equipped by one two and three impellers (Fig. 2). These configurations are defined respectively by:

$$h_1 = H/3 \tag{1}$$

$$h_1 = h_2 = H/3 \tag{2}$$

$$2h_1 = h_2 = h_3 = H/3 \tag{3}$$

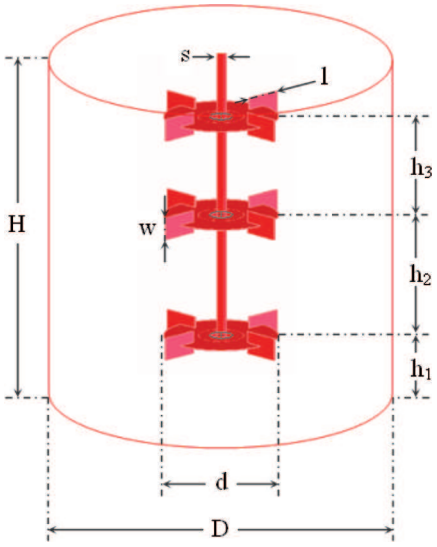

Fig. 1. Multiple four-blade Rushton impellers

Fig. 2. Stirred vessel configurations

3. Numerical model

To compare the fundamental mechanisms of laminar mixing with multiple Rushton impellers in a vessel tank, a specific computational fluid dynamics (CFD) code is developed [19-25].

3.1 Navier-Stokes equations

The simulation of the laminar flow field of the multi-Rushton impellers in a stirred tank is governed by Navier-Stokes equations. For incompressible fluids, the continuity equation is given in the following form:

$$\frac{\partial \mathrm{U}}{\partial r}+\frac{1}{\mathrm{r}}\frac{\partial \mathrm{V}}{\partial \theta}+\frac{\partial \mathrm{W}}{\partial \mathrm{z}}=0 \tag{4}$$

The momentum equations are written in a rotating reference frame. Therefore, the centrifugal and the Coriolis accelerations terms are added. These equations, written in cylindrical coordinates (r,θ,z), are expressed in the general conservation form. For the radial compound, we can write:

$$\frac{\partial \mathrm{U}}{\partial \mathrm{t}}+\mathrm{div}\left[\vec{V}\,\mathrm{U}-\frac{2}{\pi}\left(\frac{\mathrm{d}}{\mathrm{D}}\right)^2\frac{1}{\mathrm{Re}}\eta\,\overrightarrow{\mathrm{grad}}\mathrm{U}\right]=$$

$$=-\frac{\partial \mathrm{p}}{\partial \mathrm{r}}+\frac{2}{\pi}\left(\frac{\mathrm{d}}{\mathrm{D}}\right)^2\frac{1}{\mathrm{Re}}\left[\begin{array}{l}-2\eta\left[\dfrac{\mathrm{U}}{\mathrm{r}^2}+\dfrac{1}{\mathrm{r}^2}\dfrac{\partial \mathrm{V}}{\partial \theta}\right]+\dfrac{1}{\mathrm{r}}\dfrac{\partial}{\partial \mathrm{r}}\left[\mathrm{r}\,\eta\dfrac{\partial \mathrm{U}}{\partial \mathrm{r}}\right]\\ \\ +\dfrac{\partial}{\mathrm{r}\,\partial\theta}\left[\eta\,\mathrm{r}\,\dfrac{\partial}{\partial \mathrm{r}}\left(\dfrac{\mathrm{V}}{\mathrm{r}}\right)\right]+\dfrac{\partial}{\partial \mathrm{z}}\left[\eta\dfrac{\partial \mathrm{W}}{\partial \mathrm{r}}\right]\end{array}\right]+\frac{\mathrm{V}^2}{\mathrm{r}}+\mathrm{r}+2\,\mathrm{V} \tag{5}$$

For the tangential compound, we can write:

$$\frac{\partial \mathrm{V}}{\partial \mathrm{t}}+\mathrm{div}\left[\vec{V}\mathrm{V}-\frac{2}{\pi}\left(\frac{\mathrm{d}}{\mathrm{D}}\right)^2\frac{1}{\mathrm{Re}}\eta\overrightarrow{\mathrm{grad}}\mathrm{V}\right]=$$

$$=-\frac{\partial p}{r\partial\theta}+\frac{2}{\pi}\left(\frac{\mathrm{d}}{\mathrm{D}}\right)^2\frac{1}{\mathrm{Re}}\left[\begin{array}{l}\eta\left[\dfrac{1}{r^2}\dfrac{\partial u}{\partial\theta}+\dfrac{\partial}{\partial r}\left(\dfrac{V}{r}\right)\right]+\dfrac{1}{r}\dfrac{\partial}{\partial r}\left[\eta\left(\dfrac{\partial U}{\partial\theta}-V\right)\right]\\ \\ +\dfrac{\partial}{r\,\partial\theta}\left[\eta\left(\dfrac{\partial V}{r\,\partial\theta}+\dfrac{2U}{r}\right)\right]+\dfrac{\partial}{\partial z}\left[\eta\dfrac{\partial W}{r\,\partial\theta}\right]\end{array}\right]-\frac{UV}{r}-2U \tag{6}$$

For the axial compound, we can write:

$$\frac{\partial W}{\partial t}+\mathrm{div}\left[\vec{V}W-\frac{2}{\pi}\left(\frac{d}{D}\right)^2\frac{1}{Re}\eta\,\overrightarrow{\mathrm{grad}}W\right]=$$

$$=-\frac{\partial p}{\partial z}+\frac{2}{\pi}\left(\frac{d}{D}\right)^2\frac{1}{Re}\left[\begin{array}{l}\frac{1}{r}\frac{\partial}{\partial r}\left[r\,\eta\frac{\partial U}{\partial z}\right]+\frac{\partial}{r\,\partial\theta}\left[\eta\frac{\partial V}{\partial z}\right]\\ \\ +\frac{\partial}{\partial z}\left[\eta\frac{\partial W}{\partial z}\right]\end{array}\right]+\frac{1}{Fr} \tag{7}$$

3.2 Numerical method

The equations system has been solved using the three-dimensional CFD code developed in our Laboratory [19-25]. This code is based on solving the continuity and the Navier-Stokes equations using a finite volume method. The transport equations are integrated over its own control volume using the hybrid scheme discretization method. The discretized equations were solved iteratively using the SIMPLE algorithm for pressure-velocity coupling [26]. The algebraic equation solutions were obtained in reference to the fundamental paper published by Douglas and Gunn [27]. The discretization method and numerical solution procedure used have been described in detail elsewhere [24-25].

For the meshing, we have used the design software Solid-Works to construct the impeller shape. Then, we can define a list of nodes belonging to the interfacing, separating the solid domain from the flow domain. Using this list, the meshes in the flow domain are automatically generated for the three-dimensional simulations. Therefore, the region to be modeled is subdivided into a number of control volumes defined on a cylindrical coordinates system (r,θ,z). A staggered mesh is used in such a way that four different control volumes are defined for a given node point, one for each of the three vector components and one for the pressure. The flow field was computed using a grid size of Nr=30, Nθ =60 and Nz=60. The solution was obtained when the total residuals for the equations dropped to below 10^{-6}.

3.3 Boundary conditions

To simplify calculation and to avoid re-meshing, a steady flow field on the rotating frame fixed on the impellers is adopted. In these conditions, a non-slip condition on the non-moving impeller and a rotational speed on the tank walls are considered. In order to take into account the presence of the

impeller, all radial as well as tangential and axial velocity mesh nodes, which intersect with impeller, were taken equal to zero:

$$U(i, j, k) = 0 \tag{8}$$

$$V(i, j, k) = 0 \tag{9}$$

$$W(i, j, k) = 0 \tag{10}$$

However, at the internal wall tank we have to set the angular velocity component equal to the rotating speed because of the rotating frame:

$$V(Nr - 1, j, k) = -1 \tag{11}$$

Also, all radial as well as axial velocity mesh nodes were taken equal to zero:

$$U(Nr - 1, j, k) = 0 \tag{12}$$

$$W(Nr - 1, j, k) = 0 \tag{13}$$

When the vortex phenomenon is absent, the liquid surface of the stirred tank can be considered as plane. This is warranted because Coriolis forces are reduced due to a decrease of the tangential motion. In these conditions, we can write:

$$\frac{\partial U}{\partial z}(\mathrm{i,j,Nz\text{-}1}) = 0 \tag{14}$$

$$\frac{\partial V}{\partial z}(\mathrm{i,j,Nz\text{-}1}) = 0 \tag{15}$$

$$W(i, j, Nz - 1) = 0 \tag{16}$$

At the boundary, where the fluid leaves the computational domain, zero velocity gradients are assumed.

3.4 power consumption

The power P consumed by the impellers in the stirred tanks is equal to the power dissipated in the liquid. It was calculated from the volume integration predicated from the CFD code [2]. In the laminar flow, the total power consumption was calculated from the general relationship:

$$P = \int_{vc} \mu \, \Phi_v \, dv \tag{17}$$

Where Φ_v is the viscous dissipation rate, which can be expressed in cylindrical coordinates in the following form:

$$\Phi_v = \left[2\left[\left(\frac{\partial U}{\partial r}\right)^2 + \left(\frac{\partial V}{r\partial\theta} + \frac{U}{r}\right)^2 + \left(\frac{\partial W}{\partial z}\right)^2\right] + \left[\frac{\partial V}{\partial r} - \frac{V}{r} + \frac{\partial U}{r\partial\theta}\right]^2 + \left[\frac{\partial W}{r\partial\theta} + \frac{\partial V}{\partial z}\right]^2 + \left[\frac{\partial U}{\partial z} + \frac{\partial W}{\partial r}\right]^2\right] \tag{18}$$

The dimensional analysis enables us to characterize power consumption in a stirred tank through the power number Np [2] is defined as follows:

$$Np = \frac{P}{\rho N^3 d^5} \tag{19}$$

4. Numerical results

The hydrodynamics results, such as the flow patterns and the viscous dissipation rate are presented below. The flow conditions are defined by the Reynolds number Re = 14 and the Froude number Fr = 0.19.

4.1 Flow patterns

4.1.1 Flow patterns in r-θ plane

Figure 3 shows a velocity vector plot of the primary flow in $r-\theta$ plane defined by the axial coordinate equal to z =0.6. For the symmetry reasons, these results, relative to the three configurations already definite, are presented only on a sector equal to 90°. In these conditions, the blade is defined by an angular position equal to θ =45°. According to these results, it appears that the flow is strongly dominated by the tangential component. Far from the region swept by the impellers, the rotating movement is no longer transmitted to the fluid, which remains quasi motionless.

4.1.2 Flow patterns in r-z planes

Figures 4, 5 and 6 show the secondary flow in three different $r-z$ planes. These planes are defined respectively by the angular coordinates equal to θ = 40°, θ = 45° and θ = 85°. In these conditions, the second presentation plane is confounded with the impeller blade. However, the first and the last are situated respectively in the upstream and in the downstream of the blade plane. In the case of the one impeller, the distribution of the field velocity

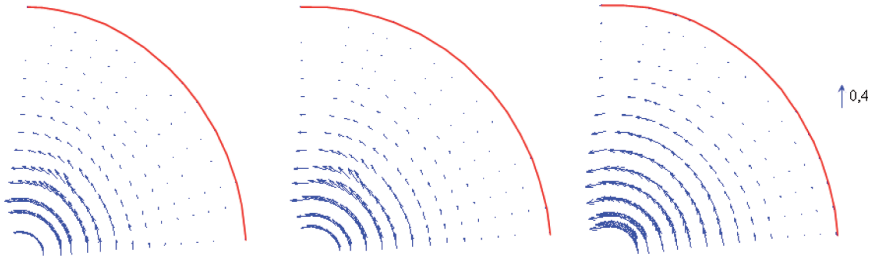

(a) One impeller (b) Two impellers (c) Three impellers

Fig. 3. Flows patterns induced in r-θ plane defined by z=0.6

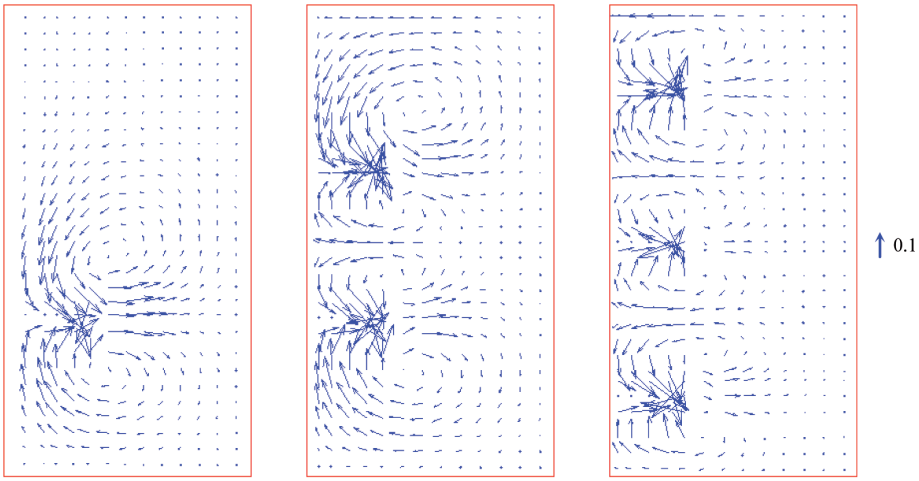

(a) One impeller (b) Two impellers (c) Three impellers

Fig. 4. Flows patterns induced in r-z plane defined by θ = 40°

shows the presence of a radial jet on the level of the turbine which changes against the walls of the tank with two axial flows thus forming two zones of recirculation on the two sides of the turbine. Also, it's noted a slowing of the flow far from the Rushton impeller. However, with two Rushton impellers there is generation of four zones of symmetrical recirculation, where slowing is lesser than the precedent configuration. The three Rushton impellers are characterized by generation of six symmetrical recirculation zones. For this system, the field of velocity is more active than the two other cases; the weak flow zones are less frequent. These results confirm that the multi-impellers systems appear necessary to decrease the weak flow zones in the stirred tanks. In these conditions, two Rushton impellers are obviously enough to improve the mechanical agitation operation. In fact, the recirculation zones appear more developed (Fig. 6.b). In this figure, for the large recirculation zones, the two recirculation centres are situated in the radial position equal to r=0.46. The two axial positions are equal to z=0.48 and z=1.56. The small

recirculation zones approach to the impeller shaft. In fact, the radial position of the recirculation centre decreases and becomes equal to r=0.26. In this case, the axial positions are equal to z=0.84 and z=1.16.

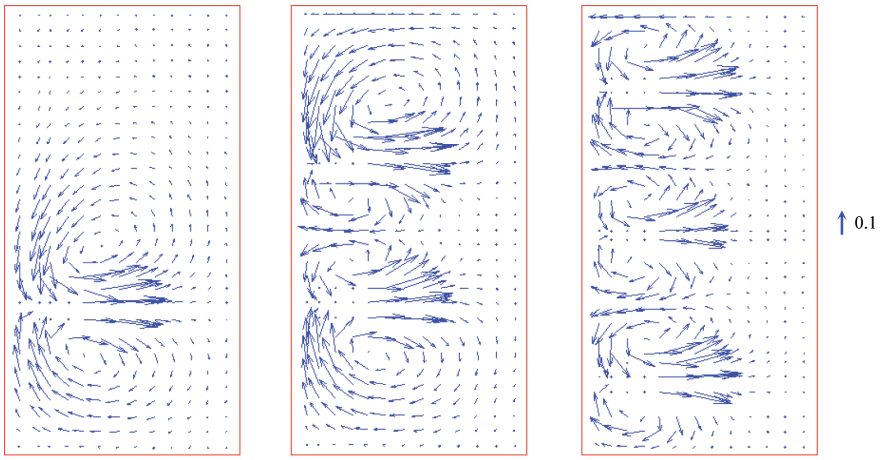

(a) One impeller (b) Two impellers (c) Three impellers

Fig. 5. Flows patterns induced in r-z plane defined by θ = 45°

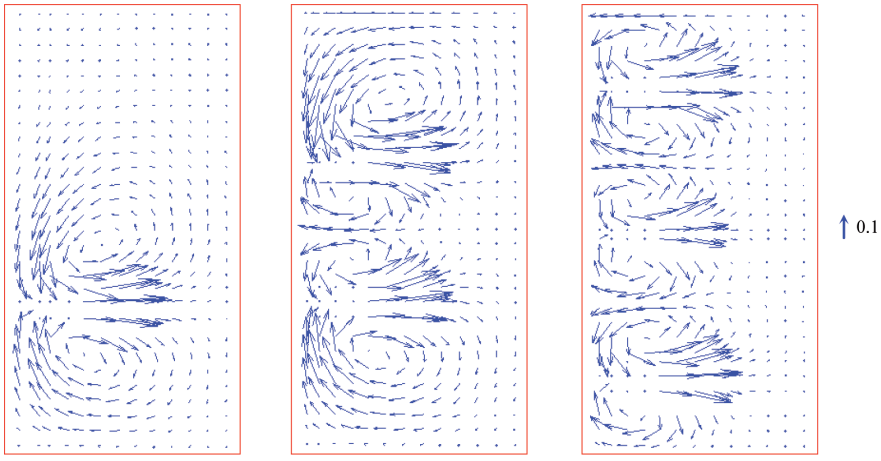

(a) One impeller (b) Two impellers (c) Three impellers

Fig. 6. Flows patterns induced in r-z plane defined by θ = 85°

4.2 Viscous dissipation rate

Figures 7, 8, 9, 10 and 11 show the viscous dissipation rate in the r-θ planes defined respectively by the axial coordinates equal to z=0.33, z=0.66,

z=1, z=1.33 and z=1.66. Figure 12 shows the viscous dissipation rate in the r-z plane defined by the angular coordinate equal to $\theta = 45°$. Globally, it's noted a maximal value in the blades tip. In fact, with one impeller the most important rate is reached at the plane defined by the axial coordinates equal to z=0.66 (Fig. 8). With two impellers, the axial coordinates are defined by z=0.66 and z=1.33 (Figs 8 and 10). However, with three impellers the axial coordinates are defined by z=0.33, z=1 and z=1.66 (Figs 7, 9 and 11). Out of the domain swept by impellers, the viscous dissipation rate becomes rapidely very weak. The same fact is observed in the r-z plane (Fig. 12).

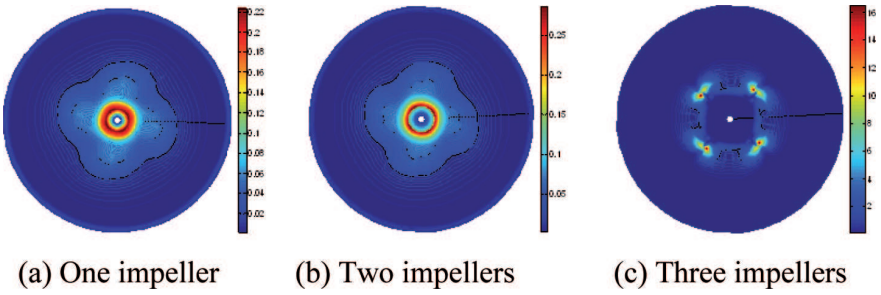

Fig. 7. Viscous dissipation rate in r-θ plane defined by z=0.33

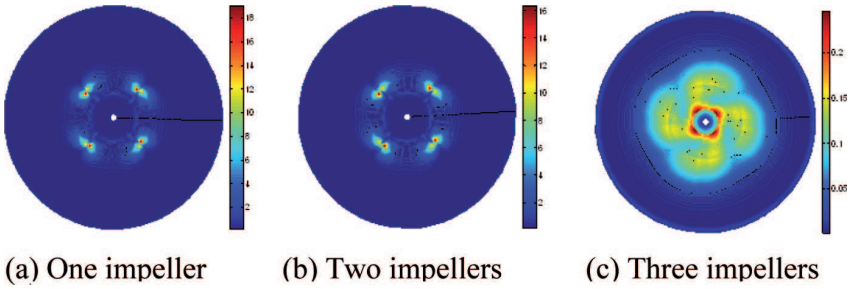

Fig. 8. Viscous dissipation rate in r-θ plane defined by z=0.66

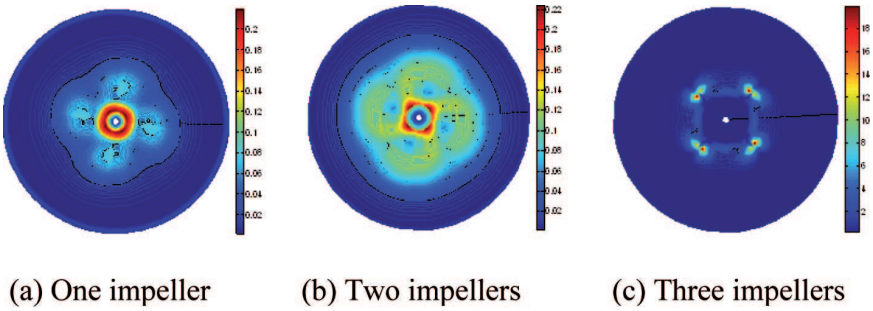

Fig. 9. Viscous dissipation rate in r-θ plane defined by z=1

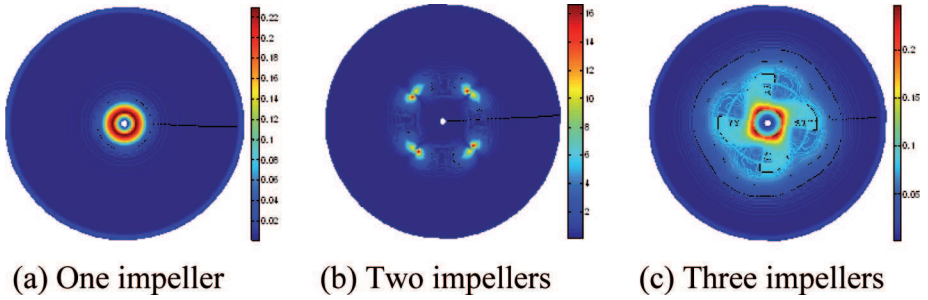

Fig. 10. Viscous dissipation rate in r-θ plane defined by z=1.33

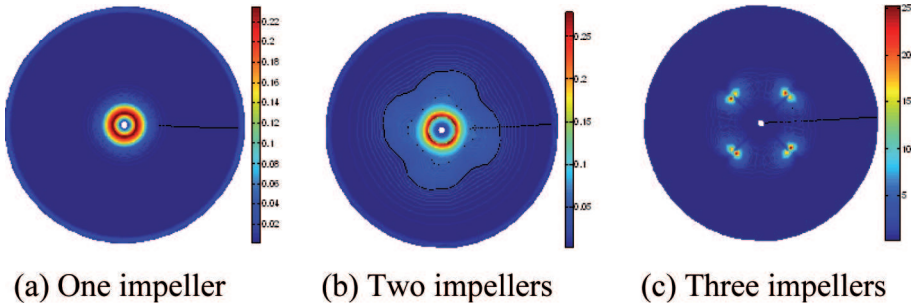

Fig. 11. Viscous dissipation rate in r-θ plane defined by z=1.66

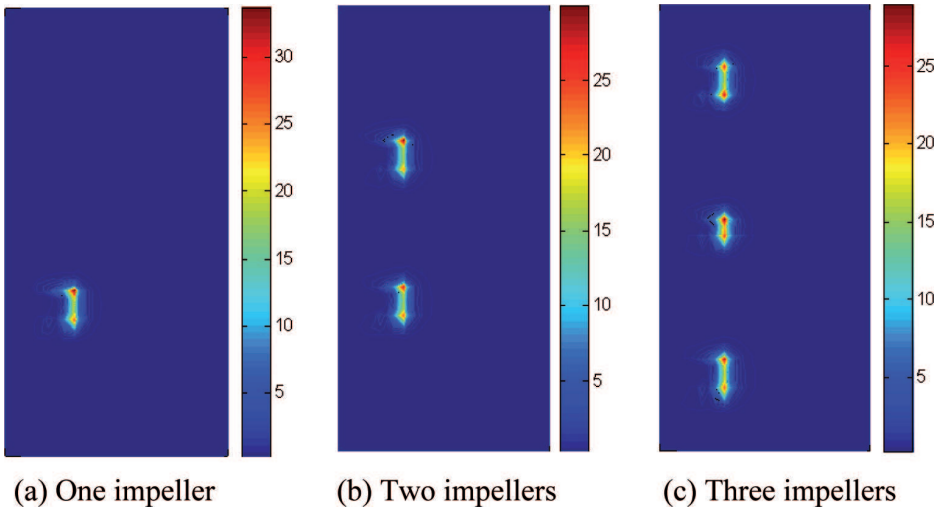

Fig. 12. Viscous dissipation rate in r-z plane defined by θ = 45°

5. Experimental results

To verify our computer results, a test bench was constructed (Fig. 13) and a methodology was elaborated. Suitable measurement was used to establish operation curves of the baffled and unbaffled stirred tanks equipped by four and six blades Rushton turbine (Fig. 14). Particularly, we are interested to measure the power of impellers in liquid of several viscosities. For the good exploitation of our test bench, we have choused an electronic regulator motor of "Heidolph" type. The motor characteristics are presented in the Table 1. This motor possesses a large range of speeds and permits the simultaneous numeric display of the rotation speed and the torque. Also, it is equipped by the RS232 interface and is piloted by the "Watch & Control" software. This software takes in load the registration of data, the graphic edition and the follow-up of the different parameters in real time. The applied manipulations were achieved in stationary regime. The test bench and the manipulations were described in detail elsewhere [25].

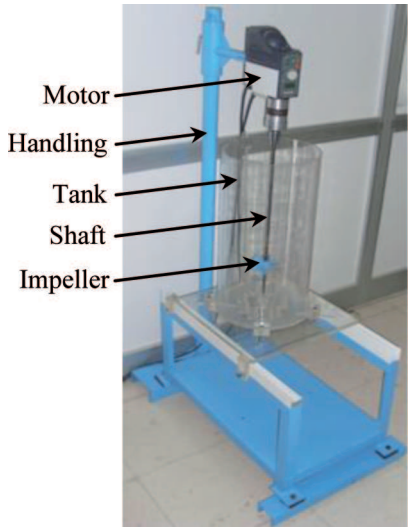

Fig. 13. Mechanical agitation test bench

(a) Four blades (b) Six blades

Fig. 14. Rushton impellers

Table 1.

Motor characteristics

Characteristics	**Value**
Maximal torque (N.m)	7
Maximal viscosity (Pa.s)	350
Maximal volume (l)	100
Speed revolution (rev.min^{-1})	Range 1 : 4-108 Range 2 : 17-540
Weight (kg)	4.7
Absorbed power (W)	140

5.1 Effect of the baffles system

Figure 15 presents the variation of the power number Np depending on the Reynolds number Re with a four-blade Rushton impeller. The experimental results correspond to a cylindrical tank with and without baffles. These curves confirm that the baffled system has a direct influence on the global results. In fact, two different zones appear in these curves. The first zone is defined by the lower Reynolds numbers and it's limited by the characteristic value of the Reynolds number noted by Re_c. In this zone, we note that the presence of the baffle doesn't have an effect on the power number. The measured values of the power number in the baffled tank are the same values obtained in the baffled tank. Beyond the characteristic value Re_c, the difference between the two curves is clear. In fact, with a baffled tank the power number Np increased. However, Np decreased without baffles. According to these results, we can confirm that the baffled tank present the mush greater

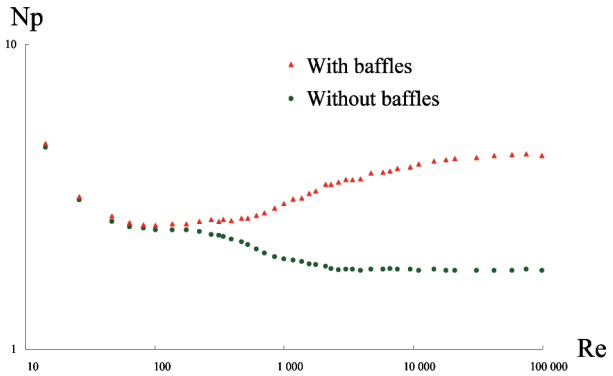

Fig. 15. Variation of the power number in the stirred tanks equipped by four-blade Rushton impeller

energy dissipation in turbulent flow. In these conditions, the baffles have an important role to avoid the vortex phenomena and to ameliorate the quality of the mixture. Also, it's important to note that the baffled system can be eliminated in the laminar flow because the vortex phenomena cannot appear.

5.2 Effect of the blades number

Figure 16 shows the variation of the power number Np depending on the Reynolds number Re in the baffled stirred tanks equipped by four and six-blade Rushton impellers. Globally, it's noted a resemblance between the two curves. However, it's clear that the power number Np measured in the case of the six-blade Rushton impeller is greater than the one measured in the case of the four-blade Rushton impeller. For this reason, the curve relative to the four-blade Rushton impeller is situated in the underhand. These results confirm that the power number decreases as the blades number decrease. This fact can be exploited in industrial processing where it's necessary to prepare the optimised stirring conditions. The use of the four-blade Rushton impeller can be essential in many situations of bio-reactors when it is fundamental to favourite the multiplications of such kind of bacteria and micro organism.

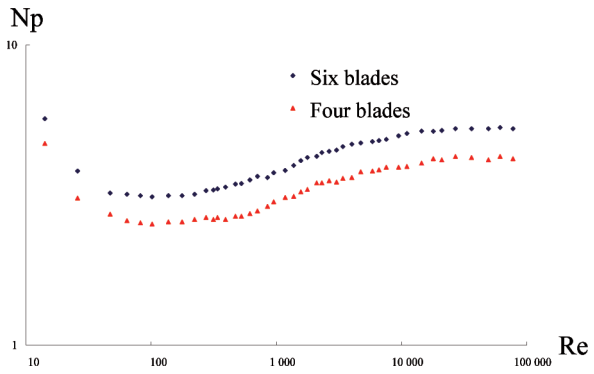

Fig. 16. Variation of the power number in the baffled stirred tanks

5.3 Comparison with anterior results

For the baffled tank equipped by a six-blade turbine, our experimental results are compared to those obtained by Rushton [28]. Globally, it's noted that we have a similar curves (Fig. 17). However, at the same Reynolds number Re, it's clear that the power number Np, measured with our test bench, is slightly lower to the experimental results done by Rushton [28]. The difference between the two results can be explained by the difference in the experimental conditions and the used instrumentations. For the unbaffled tank

equipped by a four-blade turbine, we have compared the power number value obtained by our CFD code with the experimental results. For the Reynolds number Re=14, we have found that the numerical power number is equal to 5.1 and the experimental power number is equal to 4.7. In these conditions, the relative gap is equal to 8%. These matching results indicate the validity of our computer method.

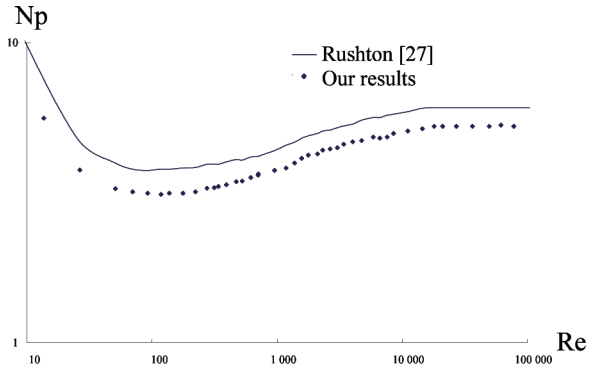

Fig. 17. Variation of the power number in the baffled stirred tanks equipped by six-blade Rushton impeller

6. Conclusion

Studying the stirred tanks is carried out to compare the fundamental mechanisms of laminar mixing with multiple Rushton impellers. Particularly, we have compared three different configurations equipped by one, two and three impellers. The gotten results confirmed that the multi-impellers systems appear necessary to reduce the amount of unreached zones in the stirred tanks. Thus, we can obviously conclude that the two Rushton impellers system is much more enough to generate an efficient mechanical agitation rather than the multiple Rushton impellers. The study of flow characteristic is greatly facilitated by modelling. The numerical results facilitate the choice of the multistage system which meets the need for each industrial application. The experimental results presented are used to validate the numerical method. This provide an excellent starting point for solid progress.

NOMENCLATURE

d	–	impeller diameter, m
D	–	internal diameter of the vessel tank, m
Fr	–	Froude number, dimensionless, $\mathrm{Fr} = \dfrac{(2\pi \mathrm{N})^2\, \mathrm{d}}{\mathrm{g}}$
g	–	gravity acceleration, $\mathrm{m.s}^{-2}$
h_1	–	position of the first impeller, m
h_2	–	position of the second impeller, m
h_3	–	position of the third impeller, m
H	–	vessel tank height, m
i	–	computational cell in radial direction, dimensionless
j	–	computational cell in tangential direction, dimensionless
k	–	computational cell in axial direction, dimensionless
l	–	blade width, m
N	–	impeller velocity, s^{-1}
N_p	–	power number, dimensionless
N_r	–	radial number nodes, dimensionless
N_z	–	axial number nodes, dimensionless
N_θ	–	angular number nodes, dimensionless
P	–	power, W
p	–	pressure, dimensionless
Re	–	Reynolds number, dimensionless, $\mathrm{Re} = \dfrac{\rho \mathrm{N d}^2}{\mu}$
r	–	radial coordinate, dimensionless
s	–	shaft diameter, m
t	–	time, s
U	–	radial velocity components, dimensionless
v	–	volume, m^3
vc	–	control volume, m^3
V	–	angular velocity components, dimensionless
w	–	blade height, m
W	–	axial velocity components, dimensionless
z	–	axial coordinate, dimensionless

$$\vec{V} = \begin{pmatrix} U \\ V \\ W \end{pmatrix} \quad - \quad \text{velocity vector}$$

Greek symbols

θ	–	angular coordinate, rad
μ	–	fluid viscosity, Pa·s
η	–	fluid viscosity, dimensionless
ρ	–	fluid density, kg·m^{-3}
Φ_v	–	viscous dissipation rate, dimensionless

Manuscript received by Editorial Board, July 22, 2011;
final version, March 03, 2012.

REFERENCES

[1] Guillard F., Tragardh C., Fuches L.: A study on the instability of coherent mixing structures in a continuously stirred tank, Chemical Engineering Science, 2000, 55, 5657-5670.
[2] Driss Z., Bouzgarrou G., Chtourou W., Kchaou H., Abid M.S.: Computational studies of the pitched blade turbines design effect on the stirred tank flow characteristics, European Journal of Mechanics B/Fluids, 2010, 29, 236-245.
[3] Kchaou H., Driss Z., Bouzgarrou G., Chtourou W., Abid M.S.: Numerical investigation of internal turbulent flow generated by a flat-blade turbine and a pitched-blade turbine in a vessel tank, International Review of Mechanical Engineering, 2008, 2, 427-434.
[4] Stitt E.H.: Alternative multiphase reactors for fine chemicals A world beyond stirred tanks, Chemical Engineering Journal, 2002, 90, 47-60.
[5] Murthy N.B., Joshi J.B.: Assessment of standard k-ε RSM and LES turbulent models in a baffled stirred agitated by various impeller designs, Chemical Engineering Science, 2008, 63, 5468-5495.
[6] Karcz J., Major M.: An Effect of a baffle Length on the power consumption in an agitated vessel, Chemical Engineering Science, 1998, 37, 249-256.
[7] Placek J., Tavlarides L.L.: Turbulent flow in stirred tanks, I: Turbulent flow in the turbine impeller region, AIChE Journal, 1985, 31, 1113-1120.
[8] Montante G., Lee K.C., Brucato A., Yianneskis M.: Experiments and predictions of the transition of the flow pattern with impeller clearance in stirred tanks, Computers and Chemical Engineering, 2001, 25, 729-735.
[9] Deglon D.A., Meyer C.J.: CFD modeling of stirred tanks: Numerical considerations, Minerals Engineering, 2006, 19, 1059-1068.
[10] Pericleous K.A., Patel M.K.: The modelling of tangential and axial agitators in chemical reactors, Physico. Chem. Hydrodyn., 1987, 8, 105-123.

[11] Costes J., Couderc J.P.: Study by laser Doppler anemometry of the turbulent flow induced by a Rushton turbine in stirred tank: influence of the size of the units, Chemical Engineering Science, 43, 1988, 2754-2772.
[12] Alcamo R., Micale G., Grisafi F., Brucato A., Ciofalo M.: Large-eddy simulation of turbulent flow in an unbaffled stirred tank driven by a Rushton turbine, Chemical Engineering Science, 2005, 60, 2303-2316.
[13] Zalc J.M., Szalai E.S., Alvarez M.M., Muzzio F.J.: Using CFD to understand chaotic mixing in laminar stirred tanks, AIChE Journal, 2002, 48, 2124-2134.
[14] Brucato A., Ciofalo M., Grisafi F., Micale G.: Numerical prediction of flow fields in baffled stirred vessels: A comparison of alternative modelling approaches, Chemical Engineering Science, 1998, 53, 3653-3684.
[15] Alvarez M.M., Zalc J.M., Shinbrot T., Arratia P.E., Muzzio F.J.: Mechanisms of mixing and creation of structure in laminar stirred tanks, AIChE Journal, 2002, 48, 2135-2148.
[16] Guillard F., Trägardh C.: Mixing in industrial Rushton turbine agitated reactors under aerated conditions, Chemical Engineering and Processing, 2003, 42, 373-386.
[17] Chtourou W., Ammar M., Driss Z., Abid M.S.: Effect of the turbulent models on the flow generated with Rushton turbine in stirred tank, Central European Journal of Engineering, 2011, 1(4), 380-389
[18] Ammar M., Driss Z., Chtourou W., Abid M.S.: Study of the baffles length effect on turbulent flow generated in stirred vessels equipped by a Rushton turbine, Central European Journal of Engineering, 2011, 1(4), 401-412.
[19] Driss Z., Karray S., Kchaou H., Abid M.S.: CFD simulation of the laminar flow in stirred tanks generated by double helical ribbons, Central European Journal of Engineering, 2011, 1(4), 413-422.
[20] Driss Z., Bouzgarrou G., Kchaou H., Abid M.S.: Computer simulation of the laminar flow in stirred tanks generated by the proximity impellers of a mono and double screws type with simple and modified profiles, Mechanics & Industries, 2011, 12, 109-121.
[21] Driss Z., Kchaou H., Baccar M., Abid M.S.: Numerical investigation of internal laminar flow generated by a retreated-blade paddle and a flat-blade paddle in a vessel tank, International Journal of Engineering Simulation, 2005, 6, 10-16.
[22] Driss Z., Karray S., Kchaou H., Abid M.S.: Computer Simulations of Fluid-Structure Interaction Generated by a Flat-Blade Paddle in a Vessel Tank, International Review of Mechanical Engineering, 2007, 1, 608-617.
[23] Bouzgarrou G., Driss Z., Abid M.S., CFD simulation of mechanically agitated vessel generated by modified pitched blade turbines, International Journal of Engineering Simulation, 2009, 10, 11-18.
[24] Driss Z., Karray S., Kchaou H., Abid M.S.: Computer simulations of laminar flow generated by an anchor blade and a Maxblend impellers, Science Academy Transactions on Renewable Energy Systems Engineering and Technology, 2011, Vol. 1, N. 3, 68-76.
[25] Driss Z.: Contribution in studies of the turbines in an agitated vessel, PhD thesis, National School of Engineers of Sfax, University of Sfax, Tunisia, 2008.
[26] Patankar S.V.: Numerical heat transfer and fluid flow, Series in Computational Methods in Mechanics and Thermal Sciences, Mc Graw Hill, New York, 1980.
[27] Douglas J., Gunn J.E.: A general formulation of alternating direction implicit methods, Num. Math., 1964, 6, 428-453.
[28] Rushton J.H., Costich E.W., Everett H.J.: Power characteristics of mixing impellers, Chemical Engineering Progress, 1950, 46, 467-476.

Badanie struktury mieszania w zbiorniku z mieszadłem w systemie wielowirnikowym z czterołopatkowymi wirnikami Rushtona

Streszczenie

W pracy badano efekt konfiguracji wielołopatkowych wirników Rushtona na hydrodynamikę i skuteczność mieszania w zbiorniku z mieszadłem. Porównano trzy konfiguracje mieszadła, zdefiniowane przez jeden, dwa lub trzy wirniki Rushtona. W artykule zaprezentowano wyniki, uzyskane przy użyciu własnego oprogramowania do obliczeń dynamiki płynów (CFD), dotyczące składników pól prędkości i szybkości dyssypacji lepkościowej. Wyniki te potwierdzają, że systemy wielowirnikowe są niezbędne dla zmniejszenia stref zubożonych w każdym zbiorniku z mieszadłem. Wyniki eksperymentalne, uzyskane w tej pracy, są porównane z wynikami obliczeń numerycznych. Dobra zgodność wyników potwierdza przydatność metody numerycznej.